energies

MDPI

Article

Thermodynamic and Economic Analyses of Zero-Emission Open Loop Offshore Regasification Systems Integrating ORC with Zeotropic Mixtures and LNG Open Power Cycle

Manuel Naveiro [1], Manuel Romero Gómez [2,*], Ignacio Arias-Fernández [2] and Álvaro Baaliña Insua [2]

[1] Energy Engineering Research Group, University Institute of Maritime Studies, Escuela Técnica Superior de Náutica y Máquinas (ETSNM), University of A Coruña, Paseo de Ronda 51, 15011 A Coruña, Spain
[2] Energy Engineering Research Group, University Institute of Maritime Studies, Nautical Sciences and Marine Engineering Department, Escuela Técnica Superior de Náutica y Máquinas (ETSNM), University of A Coruña, Paseo de Ronda 51, 15011 A Coruña, Spain
* Correspondence: m.romero.gomez@udc.es

Abstract: The present study provides an energy, exergy and economic analysis of a seawater regasification system (open loop) combining stages of simple organic Rankine cycles (ORCs) arranged in series with an open organic Rankine cycle (OC) in order to exploit the cold energy of liquefied natural gas (LNG). The proposed system, termed ORC-OC, is implemented in a Floating Storage Regasification Unit (FSRU) to achieve the objective of zero greenhouse emissions during the regasification process. Configurations of up to three stages of ORCs and the use of zeotropic mixtures of ethane/propane and n-butane/propane as working fluids are considered in the study of the novel regasification system. Only the two-stage ORC-OC (2ORC-OC) and three-stage (3ORC-OC) configurations accomplish the objective of zero emissions, attaining exergy efficiencies of 61.80% and 62.04%, respectively. The overall cost rate of the latter, however, is 20.85% greater, so the 2ORC-OC results as being more cost-effective. A comparison with conventional regasification systems installed on board shows that the 2ORC-OC yields a lower total cost rate if the LNG price exceeds 8.903 USD/MMBtu. This value could be reduced, however, if the electrical power that exceeds the FSRU's demand is exported and if compact heat exchangers are implemented.

Keywords: Floating Storage Regasification Unit; exergy analysis; economic analysis; liquefied natural gas cold energy; organic Rankine cycle

Citation: Naveiro, M.; Romero Gómez, M.; Arias-Fernández, I.; Baaliña Insua, Á. Thermodynamic and Economic Analyses of Zero-Emission Open Loop Offshore Regasification Systems Integrating ORC with Zeotropic Mixtures and LNG Open Power Cycle. *Energies* **2022**, *15*, 8622. https://doi.org/10.3390/en15228622

Academic Editors: Lazaros Aresti and Gregoris Panayiotou

Received: 11 October 2022
Accepted: 12 November 2022
Published: 17 November 2022

1. Introduction

The long-distance transport of natural gas (NG) requires that hydrocarbon be liquefied at an approximate temperature of −162 °C for optimal storage in the tanks of liquefied natural gas (LNG) carriers [1]. Import terminals, such as onshore terminals or Floating Storage Regasification Units (FSRUs), then carry out the LNG regasification process to transfer the hydrocarbon to the end users via pipelines [2]. The regasification process, provided it is not prohibited by the local authority and the ambient temperature is sufficient, is usually performed with seawater as the heat source (open loop regasification systems) [3]. Most regasification systems, however, do not recover the cold energy of the LNG, leading the scientific community to investigate its possible applications, such as power generation [4].

Most research has been focused on the utilisation of LNG cold energy as a sink in the organic Rankine cycle (ORC) [5]. The literature is extensive and there are recent reviews that include the main contributions of researchers, as in [4–8]. Most published research involving the ORC discusses different configurations that employ pure working fluids, but there are fewer investigations on zeotropic mixtures, despite the current interest that its use has aroused to improve the ORC power output [9,10]. The main contributions in

the field of LNG cold energy exploitation by means of ORCs with zeotropic mixtures are outlined below.

In recent research, Sun et al. [11] considered the use of ternary mixtures of methane, ethane (or ethylene) and propane for different configurations of a novel simple ORC. The cycle was assessed in isolation and in combination with the direct expansion of NG. Lee et al. [12] carried out a thermodynamic analysis of an ORC with a preheater, superheater, reheater and a two-stage turbine that, as well as taking advantage of the LNG cold energy, uses low-pressure steam from a pulverized coal-fired thermal plant with CO_2 capture. The proposed ORC uses a ternary mixture of n-pentane/R23/R14 and, as well as better energy and exergy efficiency, increases the power generated by 56% in comparison with pure propane. Kim et al. [13] studied the use of binary mixtures in a three-stage cascade ORC for a heat source temperature range of 25–85 °C. The working fluid compositions were optimised to minimise the exergy destroyed. The results demonstrate that the R14/propane mixture is best for the first stage, while the ethane/n-pentane mixture is best suited to the second and third stages. Lee and Mitsos [14] proposed a hybrid optimisation method (two steps) for component selection and working fluid composition of a simple ORC. The authors considered ternary mixtures in the optimisation process, obtaining the best results with a mixture of n-pentane/R23/R14. Xue et al. [15] performed an energy, exergy and economic analysis of an ORC with two stages in cascade and a third in series in which the highest temperature cascade stage provided cooling for external processes. The proposed system was compared with a cascade two-stage ORC and both configurations were assessed for a total of four cases in which pure hydrocarbons or binary and ternary mixtures of methane, ethane, ethylene and propane were used as working fluids in the different stages. Bao et al. [16] proposed a one-step optimisation method for the selection of working fluids (components and composition) and applied this to two ORCs, one of these with LNG cold energy exploitation. Both systems were simulated for pure working fluids and binary and ternary mixtures. The ORC with cold energy utilisation achieved the maximum net power for a ternary mixture of propylene/isobutane/pentane. Bao et al. [17] combined the two-stage condensation ORC with NG direct expansion and assessment ranges from pure working fluids to five-component mixtures. The net power steadily dropped as the number of components increased. Thus, the authors concluded that the maximum number of components should be limited to three. Yuan et al. [18] performed the multi-objective optimisation (net power and total cost) of two ORCs with multiple condensing stages (two and three stages) with binary and ternary mixtures, applying the ideal point method to determine the optimal design of the Pareto front. The results suggest that the optimal design for a two-stage condensation ORC is achieved with binary mixtures composed of ethane or ethylene. Tian et al. [19] performed the energy, exergy and economic analysis of a two-stage ORC in series with binary mixtures (ethane/ethylene (or propylene) in the low-temperature stage and isobutane (or n-butane)/isopentane (or n-pentane) in the high) for an LNG-powered ship. The system uses the high temperature cooling water of the dual fuel (DF) engine as a heat source in the low-temperature stage, while exhaust gases are used in the high-temperature stage. The results show that the proposed ORC reaches maximum power production with pure fluids in both stages (ethylene and isobutane), while a mixture of ethane/propylene in the low-temperature stage and pure n-butane in the high perform the best economically. Mosaffa and Garoushi [20] integrated LNG cold energy in the ORC power generation of a salt gradient solar pond and looked into several binary mixtures, obtaining the best thermodynamic results with working fluid R245ca/R236ea. He et al. [21] proposed a seawater desalination process using hydrates that exploits LNG cold energy and incorporates a simple ORC. Three pure working fluids (ethylene, ethane and R32) and a binary mixture (ethane/propane) were considered for the ORC, the latter obtaining optimal results in terms of power generation and fresh water production. He et al. [22] explored the effects of LNG vaporisation pressure, seawater temperature, minimum temperature difference and working fluid selection on the thermodynamic performance of a simple ORC. The authors assessed nine pure working fluids with their corresponding binary

combinations. The propylene/ethane mixture increased both energy and exergy efficiency by over 20% compared to the optimum pure working fluid.

In summary, the research to date on zeotropic mixtures has looked into different ORC configurations, but the most investigated has been that of the simple ORC. With regard to working fluids, ternary mixtures of hydrocarbons generally yield good thermodynamic results, although when compared with binary mixtures, the latter achieve the best economic performance. Undoubtedly, the use of LNG cold energy in ORCs with zeotropic mixtures is an area of interest and has been barely exploited considering the potential applications and advantages. More specifically, the study of its use in FSRUs is virtually non-existent.

Research on the application of the ORC with cold energy utilisation in FSRUs has focused on open loop regasification systems with ORC configurations both in series (up to three stages) [23–25] and in cascade (maximum four stages) [26,27] and the possible integration of waste heat from engine exhaust gases [28]. A summary of these works is shown in Table 1. From these studies, only Yoon-Ho in [24] considered the use of an ethane/propane zeotropic mixture for a simple ORC and the first stage of a two-stage ORC.

Table 1. Summary of previous studies on LNG cold energy utilisation in FSRUs.

Ref.	Cycle Description	Heat Source	Working Fluids	Remarks
[23]	Simple ORC	Seawater	R143a, R152a, NH_3, R134a, C_3H_6, C_3H_8	Energy and exergy analysis. The C_3H_8 offers best results for simple ORC. The 2 stage ORC with C_2H_6 (1st stage) and C_3H_8 (2nd stage) duplicates efficiency compared to the simple ORC.
	Two-stage ORC		C_2H_6, C_3H_8, R23, R116	
[24]	Simple ORC	Seawater	C_2H_6:C_3H_8	Thermoeconomic analysis. The study considers zeotropic mixtures. The best C_2H_6:C_3H_8 composition ratios for simple ORC and 2 stage ORC are 6:4 and 8:2 (only 1st stage), respectively.
	Two-stage ORC		C_2H_6:C_3H_8 (1st stage)/ C_3H_8 (2nd stage)	
[25]	Simple ORC	Seawater	C_3H_8	Thermoeconomic analysis. A regasification system with ORC and a turbine that expands the NG consumed by the engines is proposed. The 3-stage ORC w/partial expansion obtains the best results.
	Two-stage ORC		C_2H_6 (1st stage)/C_3H_8 (2nd stage)	
	Three-stage ORC		C_2H_6 (1st stage)/C_3H_8 (2nd stage) n-C_4H_{10} (3rd stage)	
	Simple ORC w/ partial expansion		C_3H_8	
	Two-stage ORC w/ partial expansion		C_2H_6 (1st stage)/C_3H_8 (2nd stage)	
	Three-stage ORC w/ partial expansion		C_2H_6 (1st stage)/C_3H_8 (2nd stage)/n-C_4H_{10} (3rd stage)	
[26]	Three-stage cascade ORC	Seawater	C_2H_4, R23, C_3H_8, C_2H_6, C_3H_6	Energy and exergy analysis. The best results are obtained with C_2H_4 (1st level), R23 (2nd level) and n-C_3H_8 (3rd level). The primary and secondary distributary cycles increase the exergy efficiency by about 4% compared to conventional cascade 3 level cycle.
	Primary distributary three-stage cascade ORC			
	Secondary distributary three-stage cascade ORC			
[27]	Three-stage cascade ORC	Seawater	C_2H_4, C_2H_6, R23, C_3H_6, C_3H_8, NH_3, R152a, iC_4H_{10}	Energy and exergy analysis. The new regasification systems add a working fluid stream to the LNG vaporizers and increase the inlet temperature of these fluids before entering the turbines. The new systems increase the exergy efficiency by 9.29 and 11.28% compared to the conventional 3- and 4-level cascade cycles, respectively.
	Four-stage cascade ORC			
	New three-stage cascade ORC			
	New four-stage cascade ORC			
[28]	Simple ORC	Seawater	C_3H_8	Energy and second law analysis. The use of engine exhaust gases in the 2-stage ORC increases the electrical power production by 24 and 11% compared to the simple ORC and 2-stage ORC, respectively.
	Two-stage ORC		C_3H_8 (1st stage)/C_3H_8 (2nd stage)	
	Two-stage ORC	Seawater and exhaust gases	C_3H_8 (1st stage)/C_3H_8, R134a, R245fa (2nd stage)	

As discussed above, the study of zeotropic mixtures for FSRUs covers the simple ORC and the first stage of the two-stage ORC but does not include the second stage or the possibility of further stages. In addition, none of the works published to date contemplated the effect of including the ORC on the electric power balance of the vessel [29]. That is, the reduced load on the DF engines and, consequently, reduced greenhouse gas emissions associated with fuel consumption. Moreover, no study considered the combination of the open Rankine cycle (OC) with the usual ORC architectures. While in the latter part each of the stages has its own working fluid, in the OC part of the regasified system, NG is recirculated at the beginning of the regasification process, undergoing an expansion process for the production of electrical energy and subsequent condensation with the LNG cold energy [1,30].

Considering the existing gap in the scientific literature and the need to develop new regasification systems that are more environmentally friendly, this paper presents the energy, exergy and economic analysis of a novel open loop regasification system that integrates configurations of ORCs in series with an OC. The system is designed to achieve zero greenhouse gas emissions in the FSRU during the regasification process, i.e., the cycles must meet at least the FSRU's electrical power demand. Configurations of up to three stages are considered wherein the use of zeotropic mixtures of ethane/propane is assessed to improve system efficiency, whenever possible, while seeking the best compositions. Configurations capable of meeting the zero emissions target are compared with typical regasification systems installed on board.

2. System Description

Carbon emissions connected with the regasification process of an FSRU can be estimated at design level using the Energy Efficiency Design Index (EEDI). The simplified EEDI equation for a conventional regasification system that operates in an open loop and includes a recondenser to manage the excess boil-off gas (BOG) is [31]:

$$\mathrm{EEDI}\left(\frac{\mathrm{g_{CO_2}}}{\mathrm{MJ}}\right) = \frac{\left(P_{AE} - P_{AEeff}\right) C_{FAE} SFC_{AE}}{\dot{m}_{NG}(h_{NG} - h_{LNG})}, \quad (1)$$

where P_{AE} is the power to develop from the auxiliary engines, P_{AEeff} is the net auxiliary power generated by the innovative technologies that reduce the auxiliary power, C_{FAE} is the conversion factor between fuel consumption and CO_2 emissions (g_{CO2}/g_{fuel}) for auxiliary engines, SFC_{AE} is the specific fuel consumption of the auxiliary engines, $\dot{m}_{NG}$ is the mass flow rate of NG at baseload regasification capacity, h_{NG} is the specific enthalpy of the regasified NG and h_{LNG} is the specific enthalpy of the LNG contained in the storage tanks with the composition of the regasified NG.

Considering the terms of Equation (1), CO_2 emissions during the regasification process in an FSRU operating in an open loop are due exclusively to the power production in the DF engines. Consequently, to achieve the zero emissions target, the regasification system with LNG cold energy exploitation (P_{AEeff}) must be designed to satisfy the power demand of the FSRU (P_{AE}), avoiding fuel consumption in the DF engines.

Figure 1 depicts the scheme of the proposed regasification system (ORC-OC) for a typical FSRU with the characteristics of Table S1, which combines ORCs in series with an OC to meet the electrical power demand on board the FSRU. Next, the system is described by means of the trajectories followed by the LNG and BOG therein.

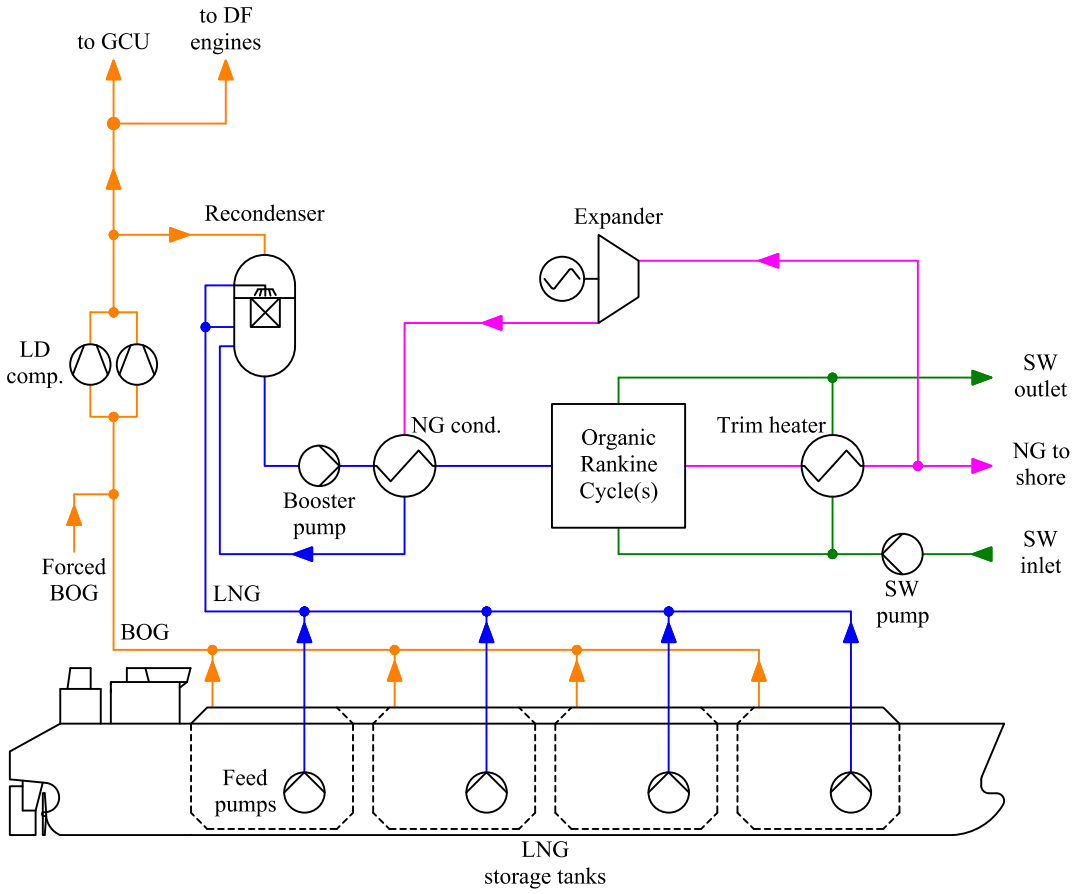

Figure 1. Simplified scheme of the ORC-OC regasification system.

Figure 2 shows the processes connected with the contribution of LNG to the regasification system, the BOG management, and the expansion and condensation of the recirculated NG in the OC. The LNG contained in the storage tank is driven by the feed pump (P-1) to the recondenser (R). Before entry, the LNG passes through the valve V-1, in which the pressure drops take place. The LNG exiting the bottom of the recondenser increases the pressure in the booster pump (P-2) before entering the NG condenser (CD-1). Next, the heated LNG increases in temperature in the condensation process of the ORC(s). As for the BOG generated in the storage tank, this is mixed with the BOG from the forcing vaporizer (FV). The latter uses the steam generated in the vessel's auxiliary boilers as the heat source and is only needed in cases where engine consumption exceeds the BOG generated in the tanks. In any case, the BOG is cooled down to a temperature of −120 °C in the mixer (MX). The cooling process is performed by spraying the LNG supplied by the fuel gas pump onto the BOG flow rate. This pump also supplies the LNG to the forcing vaporizer if required. In the separator (S), the liquid phase is removed from the cooled BOG. Next, the low duty compressor (LD) increases the pressure of the BOG coming from the separator and, subsequently, the high-pressure BOG consumed by the engines is conditioned in the after cooler/natural gas heater (AC/NGH), while the excess BOG is directed to the recondenser through the valve (V-2). If excess BOG cannot be condensed, this is burned in the Gas Combustion Unit (GCU). As the proposed system is designed to meet the electrical power demand, the flow rates of the forced BOG and BOG consumed by the engines and GCU must be zero. Lastly, the recirculated NG is expanded in the turbine (T-1) and, subsequently, condensed in CD-1 before entering the recondenser

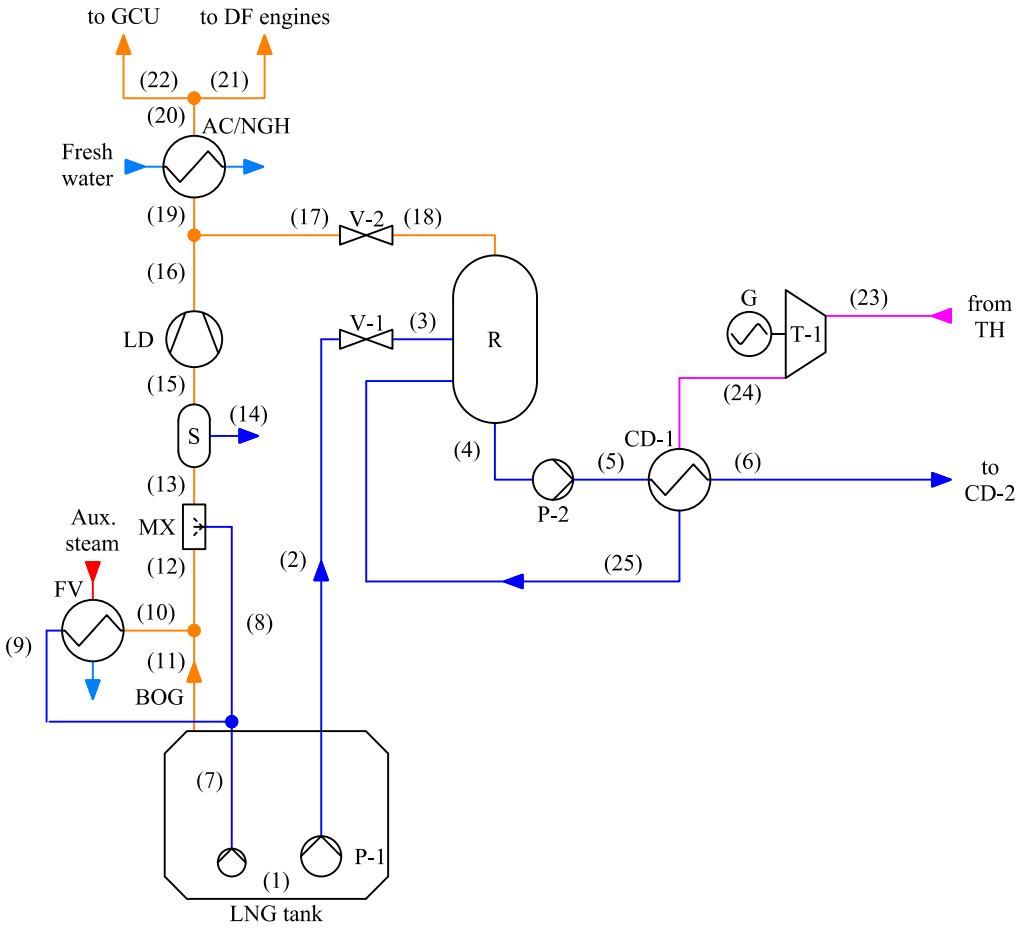

Figure 2. Diagram of the BOG handling system with LNG feed system and OC.

Figure 3 illustrates the three configurations in series considered to combine with the OC: simple ORC (1ORC, see Figure 3a), two-stage ORC (2ORC, see Figure 3b) and three-stage ORC (3ORC, see Figure 3c). Each stage has a simple ORC setup comprising a pump to increase the working fluid pressure, a vaporizer that uses seawater as a heat source and a condenser that takes advantage of the LNG cooling capacity. The seawater is delivered by the pump to each of the stages and also to the trim heater (TH). At the outlet of the latter, the NG is ready for export to the gas pipeline and part of the flow is recirculated towards T-1 for the OC operation. While the OC runs with the NG itself as the working fluid, the use of zeotropic mixtures of ethane/propane (1ORC, 2ORC and the first two stages of 3ORC) and n-butane/propane (last stage of the 3ORC) is considered in the stages in order to maximize the power produced by the cycles.

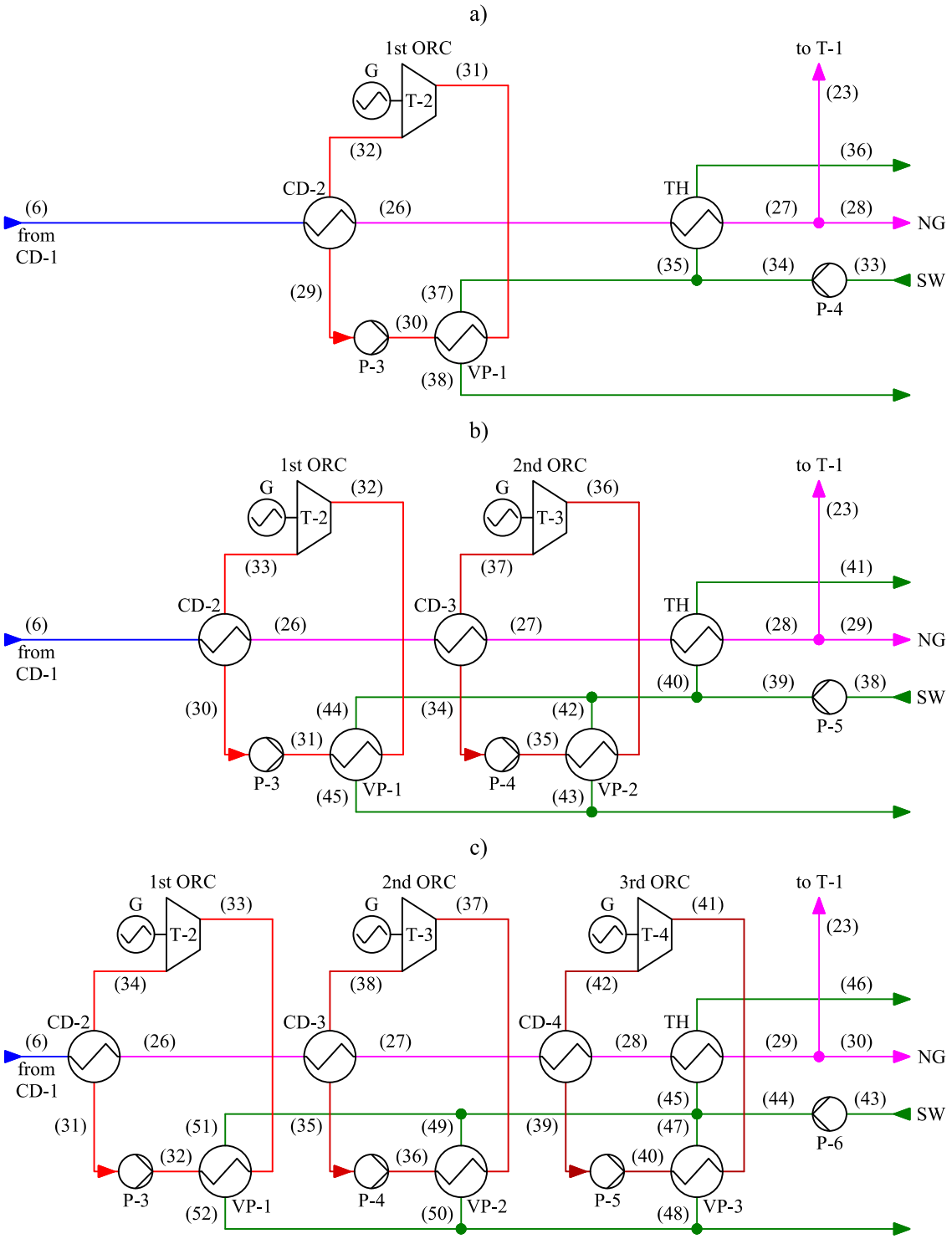

Figure 3. Arrangement of ORCs in series: (**a**) simple ORC; (**b**) two-stage ORC; (**c**) three-stage ORC.

3. Mathematical Modelling

The regasification system is modelled using a chemical process simulation software, Aspen HYSYS V11. The conditions assumed are presented below:

- The components are simulated in steady-state and adiabatic condition, neglecting the potential and kinetic effects in the energy and exergy balance equations.
- The thermodynamic properties of NG and zeotropic mixtures are determined with the Peng Robinson package. The seawater is treated as pure water, where the IAPWS-IF97 package is applied.
- Two LNG compositions are considered in the study: pure methane and the composition in Supplementary Table S2. The first one represents the reference composition and has a lower calorific value of 49,500 kJ/kg, while the second one is used for comparison purposes.
- The electrical power demand of the vessel's auxiliary services is 2050.9 kW.
- Supplementary Table S3 contains the main parameters applied.
- In the following subsections, the mathematical models and analyses developed in the study are described.

3.1. BOG Generation Calculation

A small part of the LNG stored in the tanks vaporises due to heat input from the environment. The BOG extracted from the tank ($\dot{m}_{\mathrm{BOG}}$) is determined with the following equations [31,32]:

$$\dot{m}_{\mathrm{BOG}} = \dot{m}_{\mathrm{BOG,n}} - \frac{v_{\mathrm{LNG}}}{v_{\mathrm{BOG}}}\left(\dot{m}_{\mathrm{LNG}} + \dot{m}_{\mathrm{BOG,n}}\right), \tag{2}$$

$$\dot{m}_{\mathrm{BOG,n}} = \frac{BOR\ V_{\mathrm{tk}}}{v_{\mathrm{LNG}}}, \tag{3}$$

where $\dot{m}_{\mathrm{BOG,n}}$ is the natural BOG mass flow rate, v_{LNG} is the LNG specific volume, v_{BOG} is the BOG specific volume, $\dot{m}_{\mathrm{LNG}}$ is the LNG mass flow extracted from the tank, BOR is the boil off rate and V_{tk} is the total cargo capacity.

3.2. Energy Analysis

Energy analysis involves the application of the first law of thermodynamics. The energy balance equations for pumps and compressors, turbines, valves, mixer and recondenser, phase separators and heat exchangers are, respectively:

$$\dot{W}_{\mathrm{pump/comp}} = \dot{m}(h_o - h_i), \tag{4}$$

$$\dot{W}_{\mathrm{turb}} = \dot{m}(h_i - h_o), \tag{5}$$

$$h_i = h_o, \tag{6}$$

$$\sum_i \dot{m}_i h_i = \dot{m}_o h_o, \tag{7}$$

$$\dot{m}_i h_i = \sum_o \dot{m}_o h_o, \tag{8}$$

$$\sum_i \dot{m}_i h_i = \sum_o \dot{m}_o h_o. \tag{9}$$

The FSRU electrical demand ($\dot{W}_{\mathrm{el,FSRU}}$) is determined with the following equations:

$$\dot{W}_{\mathrm{el,FSRU}} = \dot{W}_{\mathrm{el,b}} + \sum \dot{W}_{\mathrm{el,pump}} + \sum \dot{W}_{\mathrm{el,comp}}, \tag{10}$$

$$\dot{W}_{\mathrm{el,pump/comp}} = \frac{\dot{W}_{\mathrm{pump/comp}}}{\eta_{\mathrm{el,m}}}, \tag{11}$$

where $\dot{W}_{\mathrm{el,b}}$ represents the electrical consumption of the ship's auxiliary services and $\eta_{\mathrm{el,m}}$ is the electromechanical efficiency of pumps and compressors.

The sum of the power developed by each turbine ($\dot{W}_{turb}$), calculated with Equation (5), must satisfy the electrical power demand of the FSRU, as implied by the following equation:

$$\dot{W}_{required} = \dot{W}_{el,FSRU} - \sum \dot{W}_{turb}\eta_{alt} \leq 0, \quad (12)$$

where $\dot{W}_{required}$ is the required electrical power to be generated by the DF engines and η_{alt} is the efficiency of each alternator.

The energy efficiency of an FSRU can be measured based on the specific energy consumption (b_{FSRU}) with Equation (13) [33]. However, as the regasification system is designed to meet the electrical power demand, there is no BOG or pilot diesel oil (DO) consumption in the engines ($\dot{m}_{BOG}$ and $\dot{m}_{DO}$ equal to zero) and, consequently, the value of b_{FSRU} is nil.

$$b_{FSRU} = \frac{\dot{m}_{BOG}h_{LHV,BOG} + \dot{m}_{DO}h_{LHV,DO}}{\dot{m}_{NG,regasified}}. \quad (13)$$

Selection of ORC Layout and Working Fluid Composition

The zero emissions requirement during the FSRU regasification process with the ORC-OC system requires energy analysis when determining the number of stages in series and the compositions of the working fluids in each of the stages. To achieve this objective, the configurations of Figure 3 must comply with Equation (12). Therefore, these are subjected to a process of finding the optimal working fluid compositions according to Figure 4, in which the objective variable $\dot{W}_{required}$ is minimized. The process begins by entering the input parameters and simulating each configuration with pure working fluids with no recirculated NG flow rate through the OC. Next, the composition is optimized starting with the lowest order stage (from left to right) using the univariate search method [34] with a minimum step size of 0.01 in the mole fractions. The optimal compositions obtained are verified with the three-level factorial design method [34]. This method generates a grid that evaluates three levels (low, intermediate and high) for each independent variable (k), considering 3^k combinations. The grid uses the same step size as the univariate search method so that the optimal compositions must be found in the centre of the grid. Once the ORC has been optimized, the recirculated NG flow rate in the OC is adjusted to reach, if possible, zero value in the target variable. If the OC mass flow rate is high, the previously obtained values of the optimal compositions are altered. Consequently, the compositions must be re-optimized, but every time the composition changes in any working fluid, the recirculated mass flow rate of the ORC-OC must be readjusted. Considering that, at operational level, the composition of the LNG contained in the storage tanks depends on the origin of the cargo, optimisation processes are carried out for two LNG compositions: pure methane and the composition of Table S2.

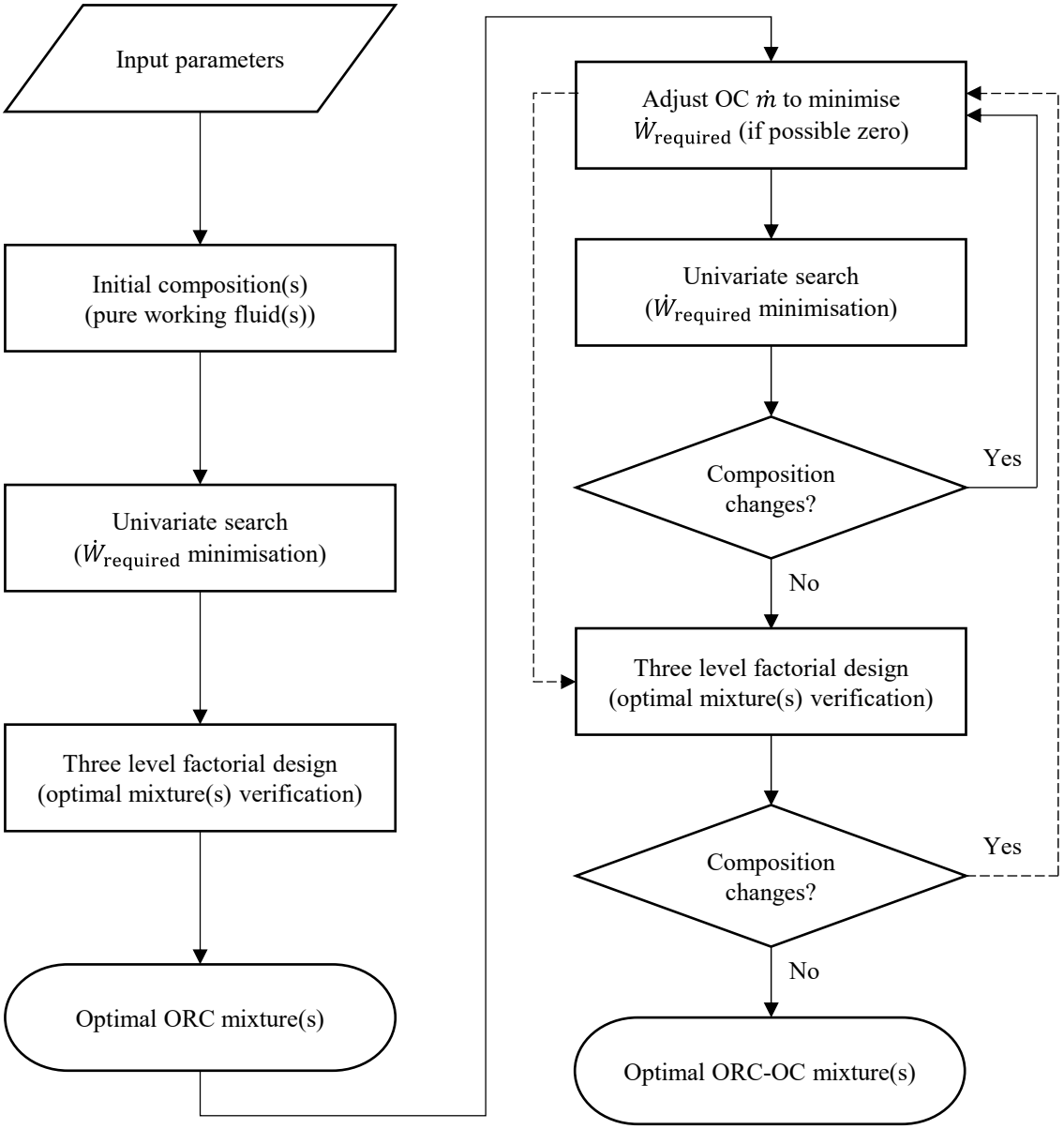

Figure 4. Methodology applied to optimise the composition of the working fluids for each system.

3.3. Exergy Analysis

Exergy analysis is a thermodynamic analysis based on the second law of thermodynamics, which determines the destruction of useful work caused by the irreversibilities of the components. In this analysis, it is necessary to explore the physical exergy terms of NG in order to define the exergy efficiency of the FSRU. Therefore, physical exergy (e^{ph}) is decomposed into a thermal (e^{th}) and a mechanical (e^{p}) component with the following equations [35]:

$$e^{ph} = h - h_0 - T_0(s - s_0), \tag{14}$$

$$e^{th} = e^{ph}(T, p) - e^{ph}(T_0, p), \tag{15}$$

$$e^{p} = e^{ph}(T_0, p) - e^{ph}(T_0, p_0), \tag{16}$$

where the terms with subscript 0 refers to the values of the same properties at the dead state.

Most of the processes that take place in the studied systems do not alter the composition of the working fluids; hence, only the chemical exergy of the NG is determined as [36]:

$$e^{\mathrm{ch}} = \varphi h_{\mathrm{LHV}}, \tag{17}$$

where φ is the NG exergy factor with a value of 1.04.

The exergy destroyed ($\dot{I}$) is determined by the exergy balance equation for each component. Equations (18)–(22) apply, respectively, to the pumps and compressors, turbines, mixer and recondenser, heat exchangers and valves.

$$\dot{I}_{\mathrm{pump/comp}} = \dot{W}_{\mathrm{pump/comp}} - \dot{m}(e_o - e_i). \tag{18}$$

$$\dot{I}_{\mathrm{turb}} = \dot{m}(e_i - e_o) - \dot{W}_{\mathrm{turb}}. \tag{19}$$

$$\dot{I}_{\mathrm{MX/R}} = \sum_i \dot{m}_i e_i - \dot{m}_o e_o. \tag{20}$$

$$\dot{I}_{\mathrm{heat\ exchanger}} = \sum_i \dot{m}_i e_i - \sum_o \dot{m}_o e_o (e_i - e_o). \tag{21}$$

$$\dot{I}_{\mathrm{valve}} = \dot{m}(e_i - e_o). \tag{22}$$

The exergy efficiency of pumps and compressors, turbines and heat exchangers are, respectively:

$$\eta_{\mathrm{ex,pump/comp}} = \frac{\dot{m}(e_o - e_i)}{\dot{W}_{\mathrm{pump/comp}}}, \tag{23}$$

$$\eta_{\mathrm{ex,turb}} = \frac{\dot{W}_{\mathrm{turb}}}{\dot{m}(e_i - e_o)}, \tag{24}$$

$$\eta_{\mathrm{ex,heat\ exchanger}} = \frac{\left[\dot{m}(e_o - e_i)\right]_{\mathrm{product}}}{\left[\dot{m}(e_i - e_o)\right]_{\mathrm{supply}}}. \tag{25}$$

Equation (25) is applicable to open heat exchangers as the mixer (precooling) and recondenser.

The exergy efficiency of each ORC stage ($\eta_{\mathrm{ex,ORC}}$) is defined as:

$$\eta_{\mathrm{ex,ORC}} = \frac{\dot{W}_{\mathrm{ORC}} - \left(\dot{E}_{\mathrm{SW,in}} - \dot{E}_{\mathrm{SW,out}}\right)}{\left(\dot{E}_{\mathrm{LNG}} - \dot{E}_{\mathrm{NG}}\right)}, \tag{26}$$

where $\dot{E}_{\mathrm{LNG}}$ is the exergy flow rate of LNG from the booster pump, $\dot{E}_{\mathrm{NG}}$ is the NG exergy flow rate at the ORC outlet and $\dot{W}_{\mathrm{ORC}}$ is the net power produced by the ORC.

The FSRU exergy efficiency based on the chemical exergy and physical exergy components of the NG can be defined as [33]:

$$\eta_{\mathrm{ex,FSRU}} = \frac{\left(\dot{E}^{\mathrm{p}}_{\mathrm{NG}} + \dot{E}^{\mathrm{p}}_{\mathrm{cond}}\right) - \left(\dot{E}^{\mathrm{p}}_{\mathrm{LNG}} + \dot{E}^{\mathrm{p}}_{\mathrm{BOG}}\right) + \dot{W}_{\mathrm{el,net}}}{\left(\dot{E}^{\mathrm{th}}_{\mathrm{LNG}} + \dot{E}^{\mathrm{th}}_{\mathrm{BOG}}\right) - \left(\dot{E}^{\mathrm{th}}_{\mathrm{NG}} + \dot{E}^{\mathrm{th}}_{\mathrm{cond}}\right) + \left(\dot{E}^{\mathrm{ch}}_{\mathrm{LNG}} + \dot{E}^{\mathrm{ch}}_{\mathrm{BOG}}\right) - \left(\dot{E}^{\mathrm{ch}}_{\mathrm{NG}} + \dot{E}^{\mathrm{ch}}_{\mathrm{cond}}\right)}, \tag{27}$$

where subscripts LNG and BOG of the equation represent the exergy flow rates associated with the LNG and BOG coming from the tank, while NG and cond subscripts are the exergy flow rates of the regasified NG and condensables collected by the mist separator. The term $\dot{W}_{\mathrm{el,net}}$ represents the power that exceeds the FSRU energy demand, if any.

3.4. Economic Analysis

The economic assessment focuses on the study of regasification modules. A module contains two booster pumps and the heat exchangers or intermediate circuit components that intervene in the LNG regasification process. In this case, as the analysis is carried out for the base regasification capacity, two identical modules of the selected architectures are proposed and a third with the characteristics of a conventional open loop propane module previously assessed in [33]. Thus, each module has a capacity of 250 mmscfd. The sizing of the heat exchangers and the evaluation of the equipment cost of each system were performed, respectively, with the Aspen EDR and APEA. The method developed in the economic assessment is described below.

The total cost rate of any regasification system installed in an FSRU ($\dot{C}_{tot}$) with zero fuel consumption is simplified to:

$$\dot{C}_{tot} = \dot{Z}_{tot}^{CI} + \dot{Z}_{tot}^{OM}, \quad (28)$$

where $\dot{Z}_{tot}^{CI}$ is the capital investment cost rate and $\dot{Z}_{tot}^{OM}$ is the operation and maintenance cost rate. The sum of these is determined as follows [37]:

$$\dot{Z}_{tot}^{CI} + \dot{Z}_{tot}^{OM} = \frac{Z_{tot}^{CI}(\gamma_{OM} + \beta_{CRF})}{\tau}, \quad (29)$$

where Z_{tot}^{CI} is the capital investment cost of the regasification system, γ_{OM} is the operation and maintenance factor, τ is the annual operating hours and β_{CRF} is the capital recovery factor. The latter is defined as:

$$\beta_{CRF} = \frac{i(1+i)^n}{(1+i)^n - 1}, \quad (30)$$

where i is the annual interest and n is the lifetime of the system.

The capital investment cost of the regasification system is updated to 2019 by means of the CEPCI with the following equation:

$$Z_{tot}^{CI} = \frac{CEPCI_{2019}}{CEPCI_{March,2018}}(FCI)_{March,2018}, \quad (31)$$

where FCI is the fixed capital investment, also known as the total project or capital cost, calculated with the APEA program and whose reference date is March 2018 [38].

The parameters assumed to calculate the total cost rate of the regasification system configurations evaluated are presented in Table 2.

Table 2. Economic analysis parameters.

Parameter	Value
γ_{OM}	3% [39]
i	12% [37]
n	20 years [25]
τ	8000 h
$CEPCI_{March,2018}$	588 [40]
$CEPCI_{2019}$	607.5 [40]

4. Results and Discussion

This section details and discusses the main results obtained from the study of the proposed regasification system with its possible configurations. Section 4.1 presents results on the selection of the number of ORC stages and the zeotropic mixture compositions in order to achieve the zero emissions objective in the FSRU. To follow, Section 4.2 sets out the relevant energy and exergy results of the configurations selected in the previous section,

while Section 4.3 details the economic results. Finally, Section 4.4 is a comparison of the chosen configurations with regasification systems studied in previous works.

4.1. ORC Layout and Working Fluid Compositions

The effects of the working fluid compositions for each ORC on the required power, simulating LNG as pure methane, are depicted in Figures 5–8. Figure 5 shows how the 1ORC is capable of reducing the required power by 45.83% in comparison with pure ethane for a molar composition ratio of ethane/propane of 76:34. Although the decrease is significant, the power required is still 1818.69 kW. In 2ORC, Figure 6 illustrates the trajectory of the optimisation process until the optimum ethane/propane composition of 94:6 is reached in the first stage and 46:54 in the second (point outlined in red). During the optimisation process, however, impossible-to-simulate compositions are reached (point with no fill) since the condensation temperature of the first stage is too high (compared to that of the second) and, consequently, a temperature difference above or equal to the minimum of 5 °C cannot be reached in the second-stage condenser. In this case, the required power drops by 87.97% compared to the situation with pure fluids, achieving a value of just 133.69 kW. In the 3ORC, the system cannot be simulated with pure n-butane in the third stage because the condensation temperature at 1.5 bar exceeds that of the vaporisation process. Therefore, the n-butane/propane mixture of the third stage is first optimized, while pure ethane and propane are used as working fluids in the first and second stages, respectively (see Figure 7). Under these conditions, the optimal value yields 948.42 kW for a 32:68 n-butane/propane ratio. As can be seen in Figure 8, the 3ORC is the only one capable of meeting the electrical power demand of the FSRU, achieving an excess of 500.55 kW for an ethane/propane ratio of 95:5 in the first stage and 47:53 in the second, while the n-butane/propane ratio in the third stage is 12:88.

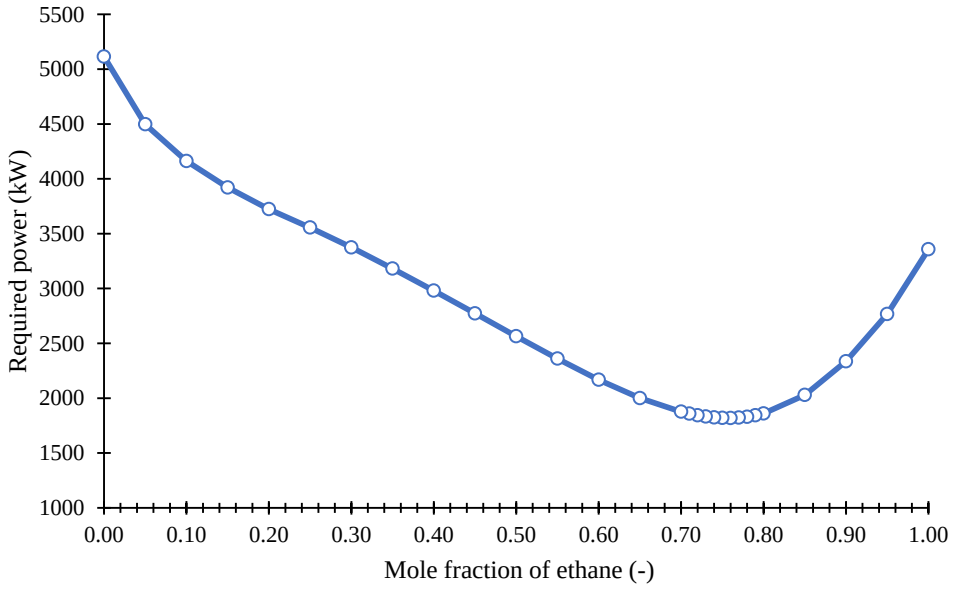

Figure 5. Effect of the working fluid composition (ethane/propane) on the required power of the 1ORC.

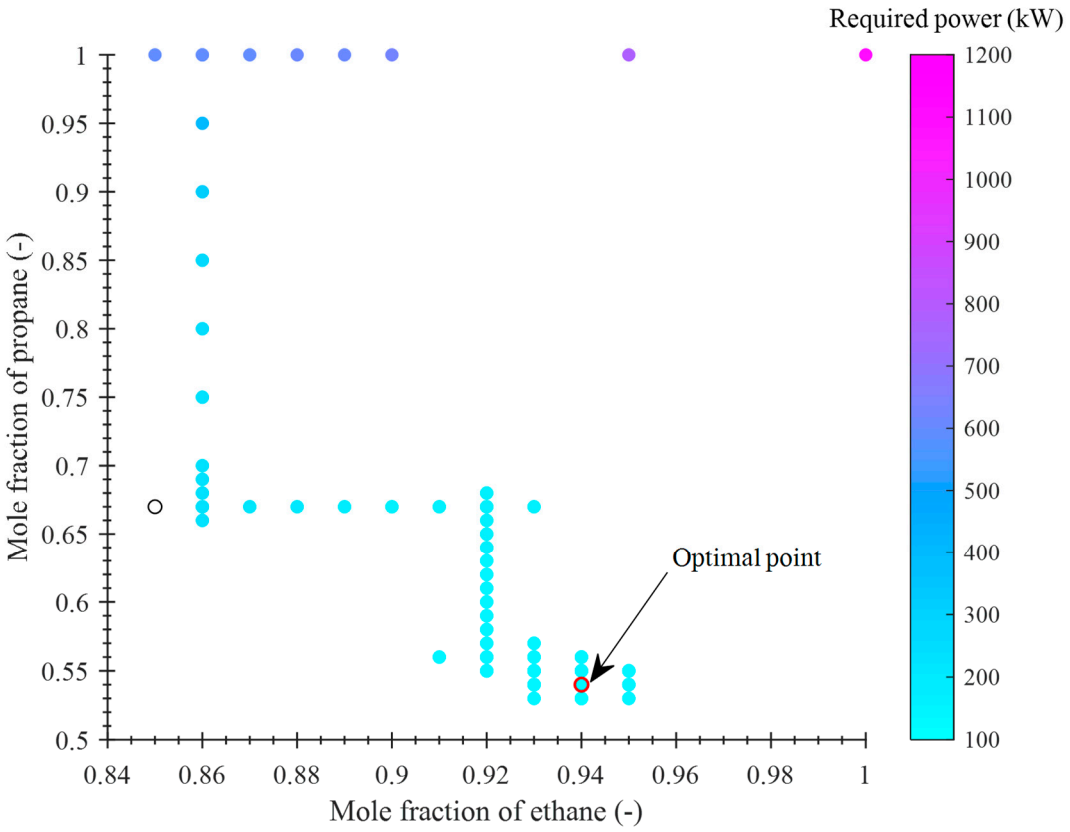

Figure 6. Effect of the working fluid composition of the 1st stage (ethane axis) and 2nd stage (propane axis) on the required power of the 2ORC in the optimisation process.

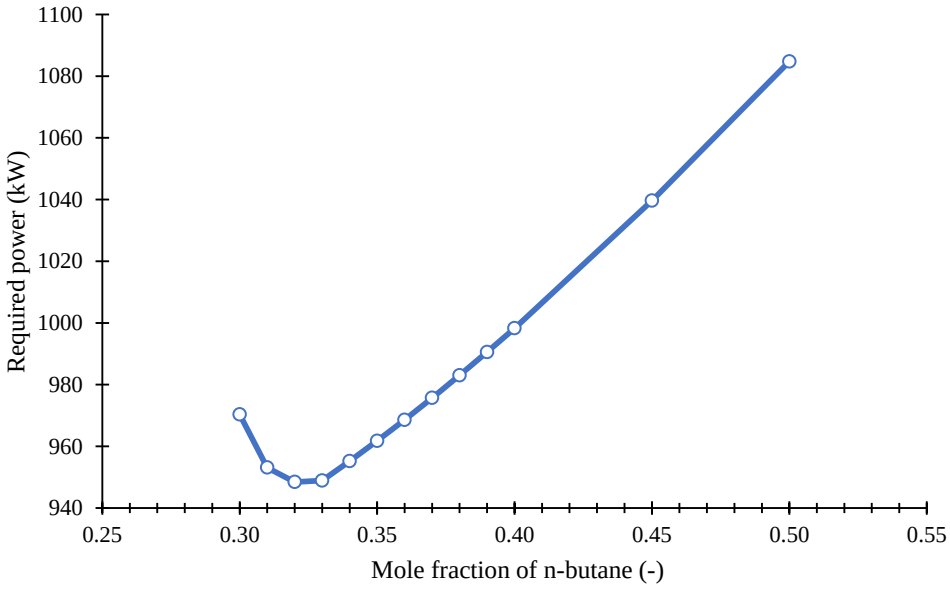

Figure 7. Effect of the working fluid composition (n-butane/propane) of the 3rd stage on the required power of the 3ORC with pure fluids in the 1st stage (ethane) and 2nd stage (propane).

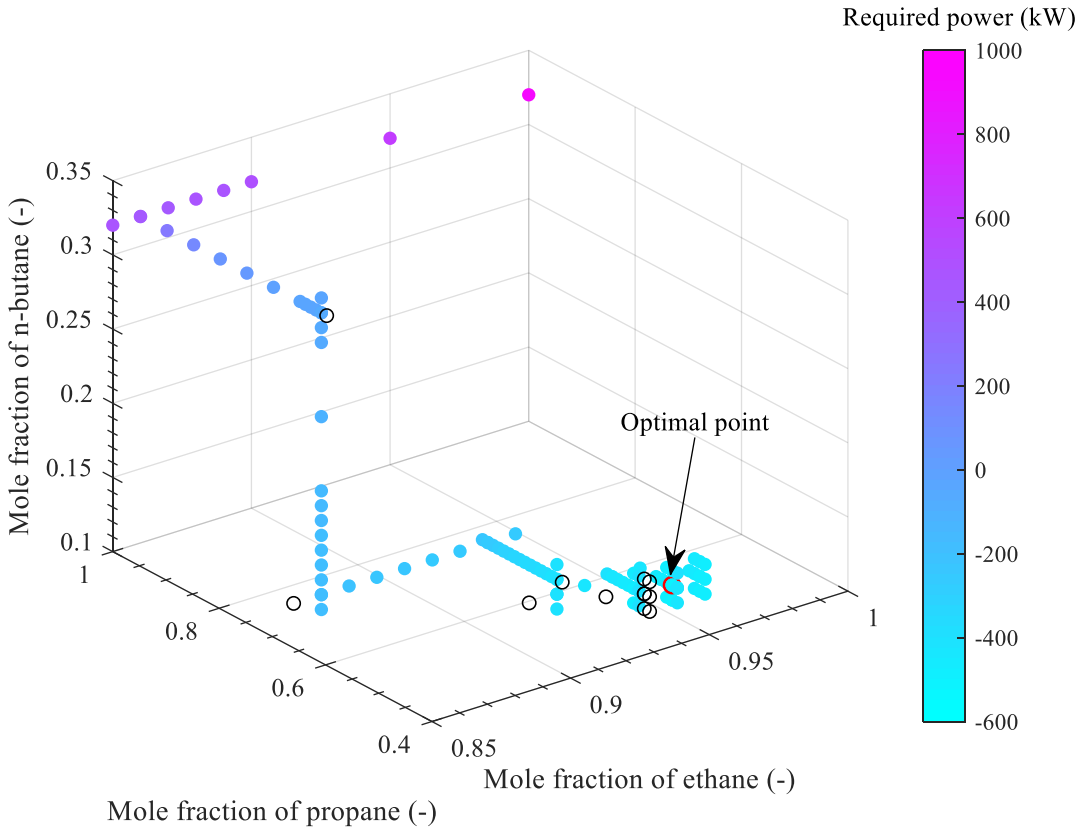

Figure 8. Effect of the working fluid composition of the 1st stage (ethane axis), 2nd stage (propane axis) and 3rd stage (n-butane axis) on the required power of the 3ORC in the optimisation process.

Supplementary Table S4, with regard to the combination of the ORCs in series with the OC and the effect of the LNG composition, presents the optimal working fluid compositions for each system, while Figure 9 depicts the required power corresponding to each. The results obtained demonstrate that the LNG composition has a significant impact on power production, with the 3ORC being unable to meet demand with the low-methane content LNG. Moreover, as can be seen in the 1ORC-OC, the maximum NG flow rate in the OC depends on the properties of this fluid in the CD-1 condensation process, with a more than double resultant value if the LNG from Supplementary Table S2 is used. In summary, there are only two cycles that can satisfy demand for a broad spectrum of LNG compositions: the 2ORC-OC and 3ORC-OC. However, while the 3ORC-OC can be simulated with pure methane using the OC mass flow rate obtained for real LNG, the same cannot be performed with that corresponding to the 2ORC-OC since such a flow rate (13.83 kg/s) exceeds the maximum possible value with pure methane (9.08 kg/s). Therefore, the 2ORC-OC is evaluated in the following sections for the maximum flow rate of the OC with optimal ethane/propane ratios of 92:8 in the first stage and 44:56 in the second.

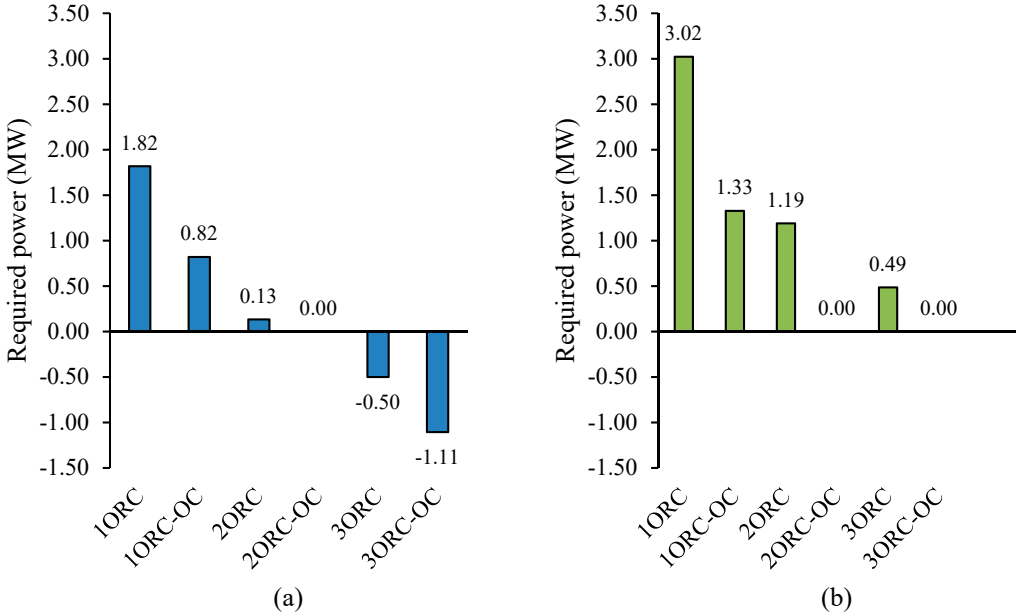

Figure 9. Effect of the LNG composition on the required power for each ORC with the optimal values: (**a**) methane; (**b**) LNG.

4.2. Thermodynamics

The main thermodynamic properties of the 2ORC-OC and 3ORC-OC states are given in Supplementary Tables S5 and S6, while Tables S7 and S8 contain the compositions. The main thermodynamic results for both configurations are presented in Table 3. The electrical power demand is slightly lower in the 2ORC-OC compared to the 3ORC-OC, just 0.20%, while production in the turbines drops to 2.41% for the first configuration. As a result, the excess power generated in the 3ORC-OC is 25.12% greater than that of the 2ORC-OC. Regarding the exergy analysis, exergy destruction in the 2ORC-OC is just 0.47% higher than that of the 3ORC-OC. Consequently, the 3ORC-OC is slightly more exergetically efficient.

Table 3. Main thermodynamic results.

Parameter	Regasification System	
	2ORC-OC	**3ORC-OC**
Electric power demand (kW)	11,299.17	11,321.46
Electric power generated (kW)	12,126.98	12,426.91
Exergy supplied (kW)	115,928.20	115,928.19
Exergy destruction (kW)	44,280.48	44,002.84
FSRU exergy efficiency (%)	61.80	62.04

Tables S9 and S10 break down the exergy destroyed and exergy efficiency for each component of the 2ORC-OC and 3ORC-OC, respectively. In both systems, the main exergy destroying component is the first stage condenser. This component accounts for 23.39% and 25.17% of exergy destruction in the 2ORC-OC and 3ORC-OC, respectively. The first stage ORC in both systems presents the highest output exergy, yet it also accounts for 43.70% (2ORC-OC) and 45.00% (3ORC-OC) of exergy losses. Thus, the second stage yields the best exergy efficiency for both systems, while the third stage in the 3ORC-OC is less efficient than the first.

4.3. Economics

A number of factors related to the design of the heat exchangers affecting the cost of the systems were considered in the economic assessment of the configurations. Titanium was the selected material for the heat exchangers in contact with seawater, while 316 L stainless steel was considered for the others. Furthermore, to reduce costs, plate heat exchangers were used in the stage vaporizers. The rest of the dimensioned heat exchangers were of shell and tube type with welded headers. Specifically, all the condensers were cross-flow (TEMA type NXN), with the exception of the NG condenser of the OC (NEN-type). The trim heater was also an NEN-type shell and tube exchanger.

Supplementary Tables S11 and S12, respectively, depict the economic results obtained from the APEA for the 2ORC-OC and 3ORC-OC, which include the itemised cost of the equipment as well as the total cost of the project. The most inexpensive configuration is the 2ORC-OC with a total cost rate of 29.94 USD/min, 20.85% lower than the 3ORC-OC. The electrical power output is greater in the 3ORC-OC, however. Therefore, in the hypothetical situation of exporting the excess power generated to land, the price of electricity needs to be at least 1.3498 USD/kWh to recompense the increase in total cost rate of the 3ORC-OC. This value is very high and unrealistic at present, although this minimum price can be reduced to 0.3390 USD/kWh if the 2ORC-OC does not export the excess power produced.

4.4. Comparison with Other Regasification Systems

The two configurations of the ORC-OC regasification system are thermodynamically compared in Figure 10 with the main systems installed in FSRUs: seawater system (SW-OL), open loop propane system (P-OL) and closed loop water–glycol system (WG-CL). These systems do not exploit the LNG cold energy of the regasification process. The comparison also includes a closed loop system with ORC and boiler flue gas CO_2 capture system (ORC-CC-CL) previously analysed in [41]. In these system, the ORC meets the electric power demand of the FSRU and the capture system treats 90% of the boiler's CO_2 emissions. Figure 10a shows the specific consumptions of each system, which are far from the zero value obtained in the ORC-OC configurations. With reference to the exergy analysis, Figure 10b depicts efficiencies of 23.60% and 24.08% above that of the seawater regasification system for the 2ORC-OC and 3ORC-OC, respectively.

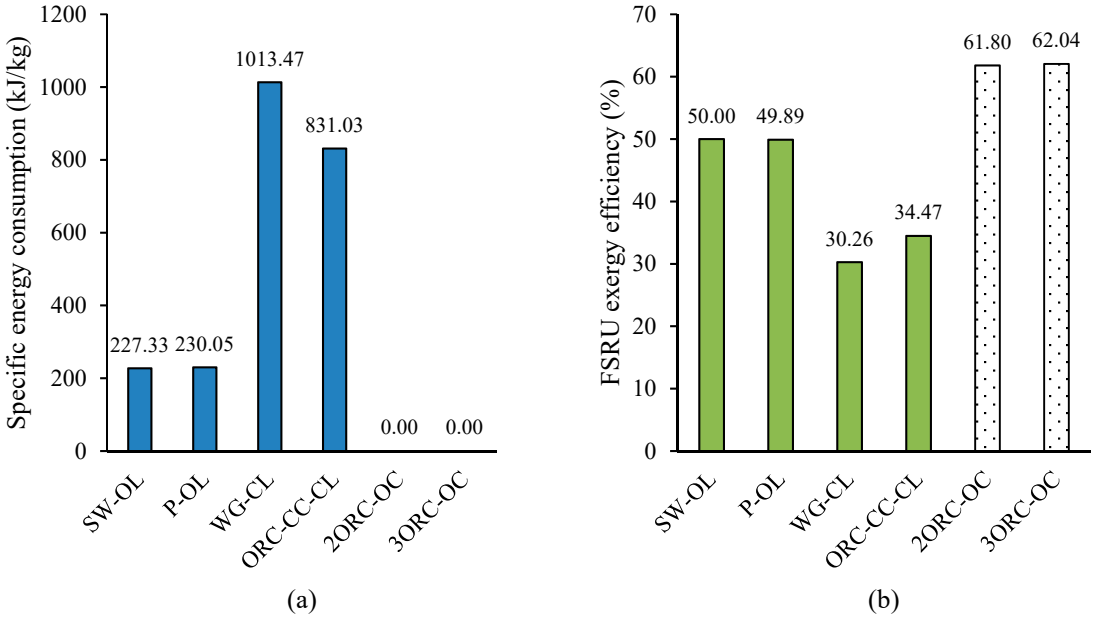

Figure 10. Comparison of the proposed regasification systems with systems of previous work [33,41]: (**a**) specific energy consumption; (**b**) FSRU exergy efficiency.

Figure 11 presents two operational indicators, the Energy Efficiency Regasification Indicator (EERI) and the Carbon Footprint Regasification Indicator (CFRI) [31], to compare CO_2 emissions per regasification energy of the FSRU of the above systems. Furthermore, two additional regasification systems are included: a seawater system without recondenser that burns excess BOG in the GCU (GCU-OL), and an open loop system with a simple ORC of propane (ORC-OL). In this case, to compare the proposed ORC-OC configurations with the other systems under the same simulation conditions, the LNG composition of Supplementary Table S2 is used. As seen in Section 4.1, the 2ORC-OC and 3ORC-OC are capable of meeting the FSRU´s power demand if the OC mass flow rate is adjusted, and, consequently, both indicators are nil for both configurations.

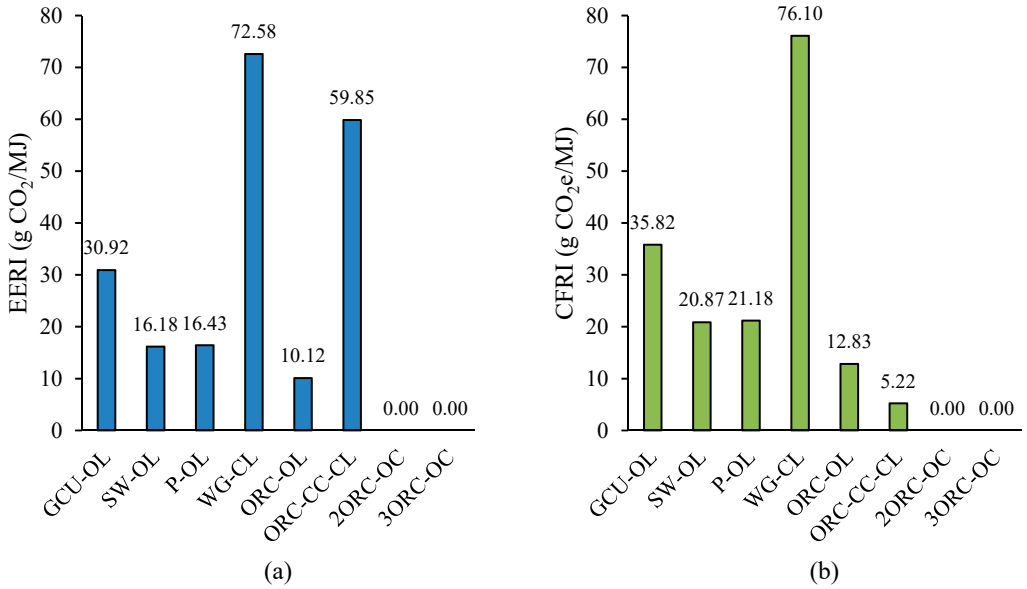

Figure 11. Comparison of the proposed regasification systems with systems of previous work [33,41]: (**a**) EERI; (**b**) CFRI.

The 2ORC-OC and 3ORC-OC are economically contrasted in Figure 12 with the three abovementioned systems installed in FSRUs. As the two configurations can meet the power demand, the total cost rate is independent of the LNG price and, hence, constant. There is, however, a threshold price of LNG to render the adoption of ORC-OC configurations more cost-effective. Considering that the open loop propane regasification system is the least expensive of the systems installed on board across a wide range of LNG prices, the point of intersection with the said system is at a price of 8.903 USD/MMBtu in the case of 2ORC-OC, and increases to 13.222 USD/MMBtu for the 3ORC-OC. These values are determined for a pilot DO price consumed by the DF engines in the open loop propane system of 500 USD/t. Figure 13 depicts how the intersection point's total cost rate varies with the interest rate, while Figure 14 indicates the price of LNG at such a point for three possible pilot fuel prices. A lower project interest rate and a higher DO price reduce the value of the LNG price at the point of intersection, particularly with the first parameter and, consequently, broaden the range of LNG prices for which it is more cost-effective to implement the ORC-OC configurations. The LNG price at the mentioned point could also be reduced by exporting FSRU excess power generation to land, or also through the implementation of compact heat exchangers in the OC and stage condensers. The latter would facilitate the installation process of such configurations since the regasification system would be significantly reduced in size.

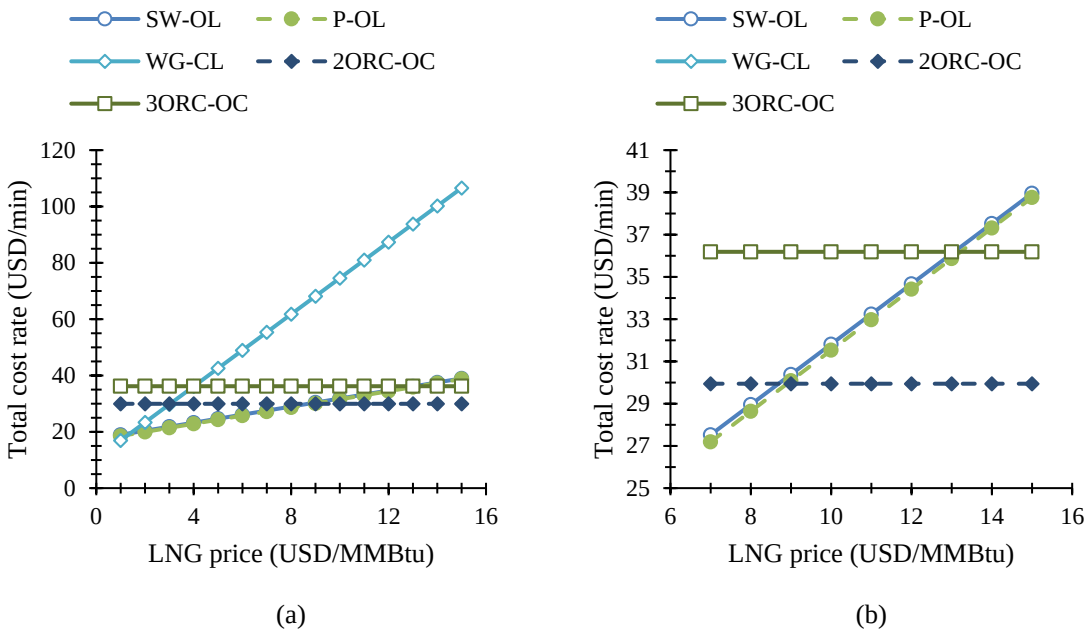

Figure 12. Comparison of the total cost rate of regasification systems as a function of the LNG price: (**a**) LNG price range 1–15 USD/MMBtu; (**b**) LNG price range 7–15 USD/MMBtu.

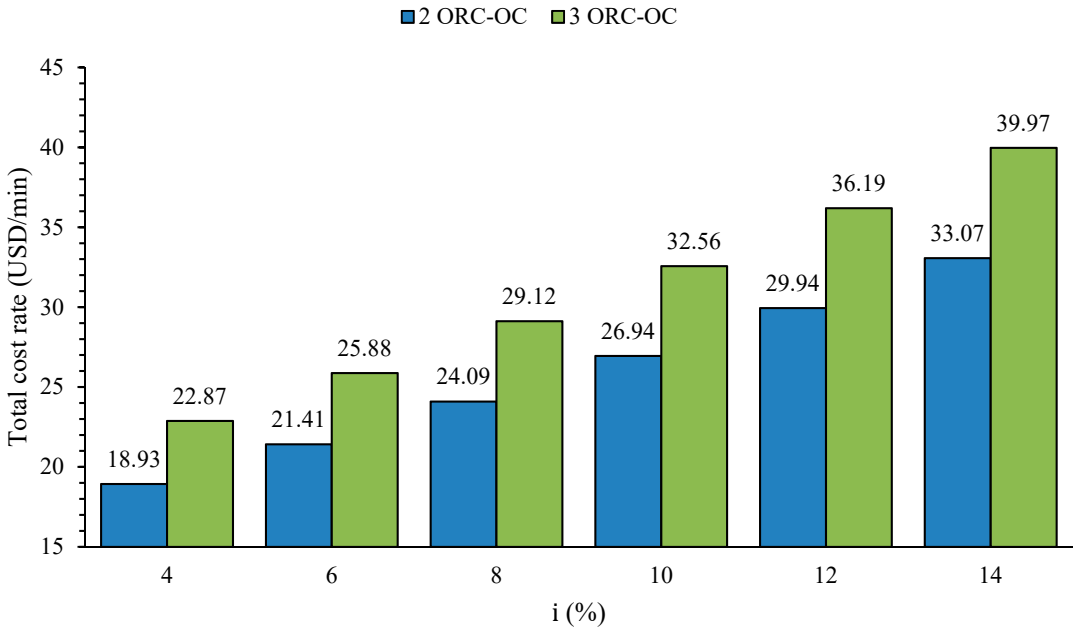

Figure 13. Effect of the interest rate on the total cost rate of the intersection point.

In summary, both configurations of the ORC-OC regasification system reduce fuel consumption to zero; that is, zero greenhouse gas emissions during the regasification process, and they significantly improve exergy efficiency in comparison with conventional regasification systems installed on board. In terms of economy, the 2ORC-OC is the most suitable configuration for installation on board since it has a lower overall cost rate and, consequently, allows for a greater range of LNG prices that render it more cost-effective than conventional regasification systems.

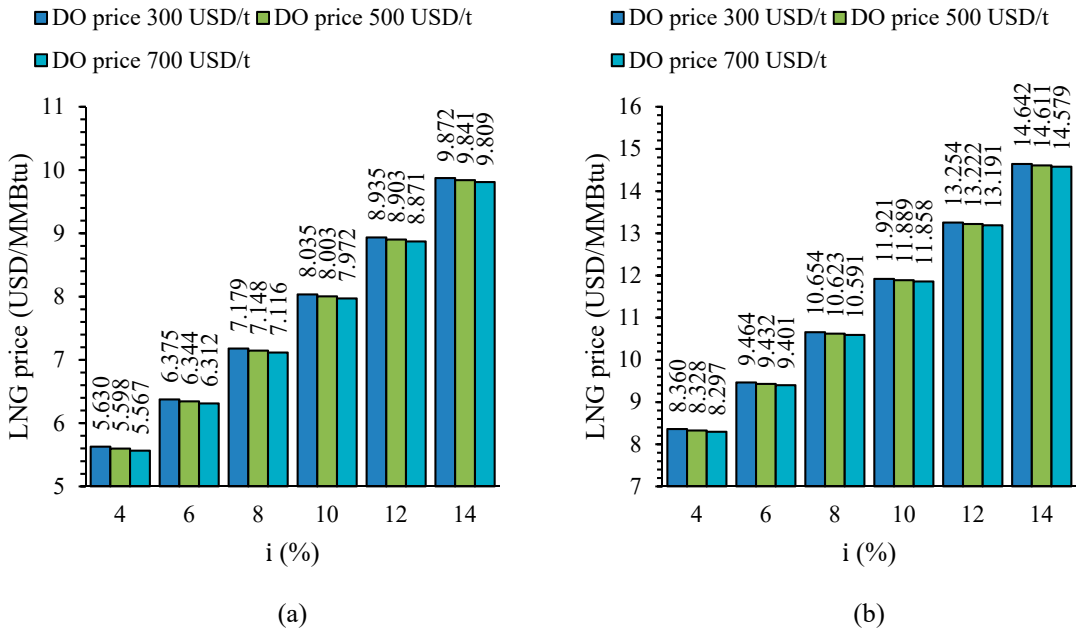

Figure 14. Effect of the DO price and interest rate on the LNG price of the intersection point: (**a**) 2ORC-OC; (**b**) 3ORC-OC.

5. Conclusions

An energy, exergy and economic analysis of an open loop regasification system for FSRUs that integrates ORCs in series with an OC in order to reduce greenhouse gas emissions to zero during the regasification process was performed herein. This combined system is referred to as ORC-OC and the main conclusions of the study are as follows:

- The zero emissions requirement in an open loop regasification system implies that DF engines cannot be used for power production. That is, the proposed system must fulfil electrical power demand through LNG cold energy exploitation.
- The arrangement of ORCs in series alone cannot satisfy the power demand for a conventional regasification capacity of 500 mmscfd. The impact of the LNG composition is considerable; hence, the ORCs in series need to be combined with an OC in order to increase electrical power production. Specifically, two configurations are able to satisfy demand with real LNG, these being the 2ORC-OC and the 3ORC-OC.
- The 3ORC-OC delivers greater surplus power than the 2ORC-OC, the values for both cases being 1105.37 kW and 827.81 kW, respectively. Regarding the exergy analysis, the 3ORC-OC renders an efficiency of 62.04%, while for the 2ORC-OC this value reduces to 61.80%. The economic analysis, however, reveals that 3ORC-OC has a greater total cost rate than the 2ORC-OC, precisely 20.85%.
- The two ORC-OC configurations are more energy efficient and environmentally friendly than regasification systems commonly installed on board. The 2ORC-OC and 3ORC-OC increase exergy efficiency by 23.60% and 24.08%, respectively, compared with the most efficient conventional regasification system; that is, the seawater system. Regarding the open loop propane regasification system, which has the lowest overall cost rate of the conventional systems for a broad range of LNG prices, the 2ORC-OC is more cost-effective if the price exceeds 8.903 USD/MMBtu, and 13.222 USD/MMBtu for the 3ORC-OC. Such values are subject to change depending on the interest rate, the price of the pilot fuel consumed by the DF engines, and on the integration of compact heat exchangers in the working fluid condensation processes.

The utilisation of LNG cold energy provides an advantageous solution to drastically cut greenhouse gas emissions during the FSRU regasification process. The development of

new open loop regasification systems that exploit cold energy is essential if the efficiency of FSRUs is to be improved and more environmentally friendly systems are to be implemented.

Supplementary Materials: The following supporting information can be downloaded at: https://www.mdpi.com/article/10.3390/en15228622/s1. Supplementary Table S1. General specifications of the model FSRU. Supplementary Table S2. NG composition measured on board an FSRU. Supplementary Table S3. General parameters assumed for the regasification system. Supplementary Table S4. Effect of the LNG composition on the optimisation variables for each power cycle. Supplementary Table S5. Thermodynamic data of the 2ORC-OC system. Supplementary Table S6. Thermodynamic data of the 3ORC-OC system. Supplementary Table S7. Composition and chemical exergy of the 2ORC-OC states. Supplementary Table S8. Composition and chemical exergy of the 3ORC-OC states. Supplementary Table S9. Exergy destruction and exergy efficiency by equipment of the 2ORC-OC system. Supplementary Table S10. Exergy destruction and exergy efficiency by equipment of the 3ORC-OC system. Supplementary Table S11. Economic results of the 2ORC-OC system obtained from the APEA. Supplementary Table S12. Economic results of the 3ORC-OC system obtained from the APEA.

Author Contributions: Conceptualization, M.N. and M.R.G.; methodology, M.N.; validation, M.N.; investigation, M.N.; writing—original draft preparation, M.N.; writing—review and editing, M.N. and M.R.G.; supervision, M.R.G., I.A.-F. and Á.B.I. All authors have read and agreed to the published version of the manuscript.

Funding: This research received no external funding.

Institutional Review Board Statement: Not applicable.

Informed Consent Statement: Not applicable.

Data Availability Statement: Not applicable.

Conflicts of Interest: The authors declare no conflict of interest.

Nomenclature

Symbols

b	specific energy consumption (kJ/kW h)
C_F	carbon factor (-)
$\dot{C}, \dot{Z}$	cost rate (USD/min)
e	specific flow exergy (kJ/kg)
$\dot{E}$	exergy flow rate (kW)
h	specific enthalpy (kJ/kg)
$\dot{H}$	energy flow rate (kW)
$\dot{I}$	irreversibilities (kW)
$\dot{m}$	mass flow rate (kg/s)
n	lifetime (years)
p	pressure (bar)
P_{AEeff}	net auxiliary power of innovative technology (kW)
$\dot{Q}$	heat transfer rate (kW)
s	specific entropy (kJ/kg-K)
SFC	specific fuel consumption (kg/kW h)
T	temperature (°C)
v	specific volume (m^3/kg)
$\dot{W}$	power (kW)

β_{CRF}	capital recovery factor (-)
γ_{OM}	operation and maintenance factor (-)
η	efficiency (-)
ρ	density (kg/m^3)
τ	annual operating hours (h)
φ	chemical exergy factor for fuels (kJ/kg)
Subscripts and Superscripts	
0	reference condition
AE	auxiliary engines
alt	alternator
b	base
ch	chemical
CI	capital investment
comp	compressor
cond	condensables
el	electrical
ex	exergy
f	fuel
i	inlet, interest
l	liquid
LHV	lower heating value
m	mechanical, mixture or mixing
n	natural
non-cond	non-condensables
o	output
OM	operation and maintenance
p	pressure
ph	physical
RS	regasification system
SW	seawater
th	thermal
Abbreviations	
AC/NGH	after cooler/natural gas heater
BOG	boil-off gas
BOR	boil-off rate
CD	condenser
CEPCI	Chemical Engineering Plant Cost Index
CFRI	Carbon Footprint Regasification Indicator
CP	centrifugal pump
DF	dual fuel
DFDE	dual fuel diesel electric
DO	diesel oil
EEDI	Energy Efficiency Design Index
EERI	Energy Efficiency Regasification Indicator
FSRU	Floating Storage Regasification Unit
FV	forcing vaporizer
GCU	Gas Combustion Unit
GCU-OL	seawater regasification system without recondenser
LD	low duty
LNG	liquefied natural gas
MX	mixer
NG	natural gas
OC	open organic Rankine cycle

ORC	organic Rankine cycle
ORC-CC-CL	close loop regasification system with ORC and carbon capture
ORC-OC	closed organic Rankine cycle with open organic Rankine cycle
ORC-OL	open loop propane regasification system with ORC
P	pump
PHE	plate heat exchanger
P-OL	open loop propane regasification system
R	recondenser
S	separator
S&T	shell and tubes heat exchanger
SW-OL	seawater regasification system
T	turbine
TH	trim heater
V	valve
VP	vaporizer
WG-CL	vclosed loop propane regasification system

References

1. Mokhatab, S.; Mak, J.Y.; Valappil, J.V.; Wood, D.A. *Handbook of Liquefied Natural Gas*; Elsevier: Amsterdam, The Netherlands, 2014; ISBN 978-0-12404-645-0.
2. Norrgård, J. *LNG Terminals-Land-Based vs. Floating Storage and Regasification Technology*; Wärtsilä: Vaasa, Finland, 2018.
3. Songhurst, B. *The Outlook for Floating Storage and Regasification Units (FSRUs)*; Oxford Institute for Energy Studies: Oxford, UK, 2017.
4. Kanbur, B.B.; Xiang, L.; Dubey, S.; Choo, F.H.; Duan, F. Cold Utilization Systems of LNG: A Review. *Renew. Sustain. Energy Rev.* **2017**, *79*, 1171–1188. [CrossRef]
5. He, T.; Chong, Z.R.; Zheng, J.; Ju, Y.; Linga, P. LNG Cold Energy Utilization: Prospects and Challenges. *Energy* **2019**, *170*, 557–568. [CrossRef]
6. Romero Gómez, M.; Ferreiro Garcia, R.; Romero Gómez, J.; Carbia Carril, J. Review of Thermal Cycles Exploiting the Exergy of Liquefied Natural Gas in the Regasification Process. *Renew. Sustain. Energy Rev.* **2014**, *38*, 781–795. [CrossRef]
7. Mehrpooya, M.; Sharifzadeh, M.M.M.; Katooli, M.H. Thermodynamic Analysis of Integrated LNG Regasification Process Configurations. *Prog. Energy Combust. Sci.* **2018**, *69*, 1–27. [CrossRef]
8. Pospíšil, J.; Charvát, P.; Arsenyeva, O.; Klimeš, L.; Špiláček, M.; Klemeš, J.J. Energy Demand of Liquefaction and Regasification of Natural Gas and the Potential of LNG for Operative Thermal Energy Storage. *Renew. Sustain. Energy Rev.* **2019**, *99*, 1–15. [CrossRef]
9. Modi, A.; Haglind, F. A Review of Recent Research on the Use of Zeotropic Mixtures in Power Generation Systems. *Energy Convers. Manag.* **2017**, *138*, 603–626. [CrossRef]
10. Xu, W.; Zhao, R.; Deng, S.; Zhao, L.; Mao, S.S. Is Zeotropic Working Fluid a Promising Option for Organic Rankine Cycle: A Quantitative Evaluation Based on Literature Data. *Renew. Sustain. Energy Rev.* **2021**, *148*, 111267. [CrossRef]
11. Sun, H.; Zhu, H.; Liu, F.; Ding, H. Simulation and Optimization of a Novel Rankine Power Cycle for Recovering Cold Energy from Liquefied Natural Gas Using a Mixed Working Fluid. *Energy* **2014**, *70*, 317–324. [CrossRef]
12. Lee, U.; Kim, K.; Han, C. Design and Optimization of Multi-Component Organic Rankine Cycle Using Liquefied Natural Gas Cryogenic Exergy. *Energy* **2014**, *77*, 520–532. [CrossRef]
13. Kim, K.; Lee, U.; Kim, C.; Han, C. Design and Optimization of Cascade Organic Rankine Cycle for Recovering Cryogenic Energy from Liquefied Natural Gas Using Binary Working Fluid. *Energy* **2015**, *88*, 304–313. [CrossRef]
14. Lee, U.; Mitsos, A. Optimal Multicomponent Working Fluid of Organic Rankine Cycle for Exergy Transfer from Liquefied Natural Gas Regasification. *Energy* **2017**, *127*, 489–501. [CrossRef]
15. Xue, F.; Chen, Y.; Ju, Y. Design and Optimization of a Novel Cryogenic Rankine Power Generation System Employing Binary and Ternary Mixtures as Working Fluids Based on the Cold Exergy Utilization of Liquefied Natural Gas (LNG). *Energy* **2017**, *138*, 706–720. [CrossRef]
16. Bao, J.; Zhang, R.; Yuan, T.; Zhang, X.; Zhang, N.; He, G. A Simultaneous Approach to Optimize the Component and Composition of Zeotropic Mixture for Power Generation Systems. *Energy Convers. Manag.* **2018**, *165*, 354–362. [CrossRef]
17. Bao, J.; Lin, Y.; Zhang, R.; Zhang, X.; Zhang, N.; He, G. Performance Enhancement of Two-Stage Condensation Combined Cycle for LNG Cold Energy Recovery Using Zeotropic Mixtures. *Energy* **2018**, *157*, 588–598. [CrossRef]
18. Yuan, T.; Song, C.; Zhang, R.; Zhang, X.; Zhang, N.; Bao, J. Energy and Economic Optimization of the Multistage Condensation Rankine Cycle That Utilizes Lng Cold Energy: Considerations on Working Fluids and Cycle Configurations. *ACS Sustain. Chem. Eng.* **2019**, *7*, 13505–13516. [CrossRef]
19. Tian, Z.; Zeng, W.; Gu, B.; Zhang, Y.; Yuan, X. Energy, Exergy, and Economic (3E) Analysis of an Organic Rankine Cycle Using Zeotropic Mixtures Based on Marine Engine Waste Heat and LNG Cold Energy. *Energy Convers. Manag.* **2021**, *228*, 113657. [CrossRef]

20. Mosaffa, A.H.; Farshi, L.G. Thermodynamic Feasibility Evaluation of an Innovative Salinity Gradient Solar Ponds-Based ORC Using a Zeotropic Mixture as Working Fluid and LNG Cold Energy. *Appl. Therm. Eng.* **2021**, *186*, 116488. [CrossRef]
21. He, T.; Zhang, J.; Mao, N.; Linga, P. Organic Rankine Cycle Integrated with Hydrate-Based Desalination for a Sustainable Energy–Water Nexus System. *Appl. Energy* **2021**, *291*, 116839. [CrossRef]
22. He, T.; Ma, H.; Ma, J.; Mao, N.; Liu, Z. Effects of Cooling and Heating Sources Properties and Working Fluid Selection on Cryogenic Organic Rankine Cycle for LNG Cold Energy Utilization. *Energy Convers. Manag.* **2021**, *247*, 114706. [CrossRef]
23. Yao, S.; Liu, H.; Tang, L.; Ye, Y.; Zhang, L. Thermodynamic Analysis and Optimization for Cold Energy Utilization Based on Low Temperature Rankine Cycle of LNG-FSRU Regasification System. *Int. J. Simul. Syst. Sci. Technol.* **2016**, *17*, 35.1–35.9. [CrossRef]
24. Yoon-Ho, L. LNG-FSRU Cold Energy Recovery Regasification Using a Zeotropic Mixture of Ethane and Propane. *Energy* **2019**, *173*, 857–869. [CrossRef]
25. Yoon-Ho, L. Thermo-Economic Analysis of a Novel Regasification System with Liquefied-Natural-Gas Cold-Energy. *Int. J. Refrig.* **2019**, *101*, 218–229. [CrossRef]
26. Yao, S.; Xu, L.; Tang, L. New Cold-Level Utilization Scheme for Cascade Three-Level Rankine Cycle Using the Cold Energy of Liquefied Natural Gas. *Therm. Sci.* **2019**, *23*, 3865–3875. [CrossRef]
27. Xu, L.; Lin, G. Simulation and Optimization of Liquefied Natural Gas Cold Energy Power Generation System on Floating Storage and Regasification Unit. *Therm. Sci.* **2021**, *25*, 4707–4719. [CrossRef]
28. Lee, S.; Choi, B.C. Thermodynamic Assessment of Integrated Heat Recovery System Combining Exhaust-Gas Heat and Cold Energy for LNG Regasification Process in FSRU Vessel. *J. Mech. Sci. Technol.* **2016**, *30*, 1389–1398. [CrossRef]
29. Naveiro, M.; Romero Gómez, M.; Arias Fernández, I.; Romero Gómez, J. Exploitation of Liquefied Natural Gas Cold Energy in Floating Storage Regasification Units. *Brodogradnja* **2021**, *72*, 47–78. [CrossRef]
30. Mak, J.Y. Configurations and Methods for Power Generation with Integrated LNG Regasification. U.S. Patent 7,574,856 B2, 18 August 2009.
31. Naveiro, M.; Romero Gómez, M.; Arias Fernández, I.; Baaliña Insua, Á. Energy Efficiency and Environmental Measures for Floating Storage Regasification Units. *J. Nat. Gas Sci. Eng.* **2021**, *96*, 104271. [CrossRef]
32. Romero Gómez, J.; Romero Gómez, M.; Lopez Bernal, J.; Baaliña Insua, A. Analysis and Efficiency Enhancement of a Boil-off Gas Reliquefaction System with Cascade Cycle on Board LNG Carriers. *Energy Convers. Manag.* **2015**, *94*, 261–274. [CrossRef]
33. Naveiro, M.; Romero Gómez, M.; Baaliña Insua, Á.; Folgueras, M.B. Energy, Exergy and Economic Analysis of Offshore Regasification Systems. *Int. J. Energy Res.* **2021**, *45*, 20835–20866. [CrossRef]
34. Edgar, T.F.; Himmelblau, D.M.; Lasdon, L. *Optimization of Chemical Processes*, 2nd ed.; McGraw-Hill: New York, NY, USA, 2001; ISBN 0-070-39359-1.
35. Frangopoulos, C.A. *Exergy, Energy System Analysis and Optimization Volume I: Exergy and Thermodynamic Analysis*; EOLSS Publications: Oxford, UK, 2009.
36. Szargut, J. *Exergy Method: Technical and Ecological Applications*; WIT Press: Southampton, UK, 2005; Volume 18, ISBN 1-85312-753-1.
37. Bejan, A.; Tsatsaronis, G.; Moran, M. *Thermal Design and Optimization*; John Wiley & Sons: Hoboken, NJ, USA, 1996; ISBN 0-471-58467-3.
38. *Aspen Technology Suite AspenONE 2019*; AspenTech: Bedford, MA, USA, 2019.
39. Querol, E.; Gonzalez-Regueral, B.; Perez-Benedito, J.L. *Practical Approach to Exergy and Thermoeconomic Analyses of Industrial Processes*; SpringerBriefs in Energy; Springer: London, UK, 2013; ISBN 978-1-4471-4621-6.
40. Chemical Engineering CEPCI Archives. Available online: https://www.chemengonline.com/tag/cepci/ (accessed on 5 September 2020).
41. Naveiro, M.; Romero Gómez, M.; Arias-Fernández, I.; Baaliña Insua, Á. Thermodynamic and Environmental Analyses of a Novel Closed Loop Regasification System Integrating ORC and CO2 Capture in Floating Storage Regasification Units. *Energy Convers. Manag.* **2022**, *257*, 115410. [CrossRef]